

Theoretical study of phase stability, electronic and magnetic properties of $\text{Rh}_2\text{CrGe}_{1-x}\text{Al}_x$ ($x = 0, 0.25, 0.50, 0.75$ and 1) Heusler alloys by FP-LAPW method

M. Kadjaoud¹, M. Mokhtari^{2,3}, L. Djoudi^{1,3}, M. Merabet^{1,3}, S. Benalia^{1,3}, D. Rached¹, R. Belacel¹, F. Zami⁴, F. Dahmane³

¹ Magnetic Materials Laboratory, Physics Department, Sidi-Bel-Abbes University, Algeria

² Université des Sciences et de la Technologie d'Oran Mohamed Boudiaf, USTO-MB, LEPM, BP 1505, El M' Naouar, 31000 Oran, Algeria

³ Département de SM, Institut des Sciences et des Technologies, Centre Universitaire de Tissemsilt, 38000 Tissemsilt, Algeria

⁴ Condensed Matter and Sustainable Development Laboratory, Physics Department, Sidi-Bel-Abbes University, Algeria

Received July 12, 2019, in final form August 29, 2019

First-principle calculations were performed within the framework of the density functional theory (DFT) using FP-LAPW method as implemented in WIEN2k code to determine the structural stability, electronic and magnetic properties of $\text{Rh}_2\text{CrGe}_{1-x}\text{Al}_x$ ($x = 0, 0.25, 0.50, 0.75$ and 1). The results showed that for Rh_2CrAl and Rh_2CrGe , the Cu_2MnAl -type structure is energetically more stable than Hg_2CuTi -type structure at the equilibrium volume. The calculated densities of states for Rh_2CrAl and Rh_2CrGe show half-metallic and nearly half-metallic behavior, respectively. $\text{Rh}_2\text{CrGe}_{1-x}\text{Al}_x$ ($x = 0.25, 0.50, 0.75$) these alloys show a half-metallic character, and these compounds are predicted to be good candidates for spintronic applications.

Key words: Heusler alloys, structural properties, electrical properties, magnetic properties

1. Introduction

Heusler alloys have been a subject of unprecedented research since their discovery in 1903 by the German engineer F. Heusler [1, 2]. The experimental works showed that the majority of Heusler alloys are ferromagnetic ordered in stoichiometric compositions [3, 4]. In the very recent past, Heusler compounds have received a great deal of interest, due to their potential applications in many fields. In particular, magnetic Heusler alloys are mostly used in spin-based electronic devices [5], thermoelectric [6, 7] and superconductors [8]. Both high-spin polarizations and half-metallicity are lately considered as the key factors in such type of materials [9, 10]. It is well known that most of Heusler alloys have the spin polarization near Fermi level which is as high as 100% [11]. Some of the Heusler alloys have only one spin channel for conduction at the Fermi level, while for the other spin channel, a semiconducting gap appears between the valence band and the conduction band [9, 12, 13].

The possibility of tuning the electronic and magnetic properties, especially the spin polarization, many of X_2YZ full, half and inverse Heusler compounds have been explored. For example, Rh_2YZ represent an interesting family in the world of Heusler compounds which has been intensively studied during the recent decades. The crystal structure and magnetic properties have been determined for a new series of compounds of the form Rh_2TSn for $T = \text{Mn, Ni, or Cu}$ [11]. In their work, M. Pugaczowa-Michalska and A. Jezierski *et al.* studied the magnetic properties of Rh_2TSn Heusler alloys ($T = \text{Mn, Fe, Co, Ni}$ and Cu) [14]. Mohammed El Amine Monir *et al.* studied half-metallic ferromagnetism in the novel Rh_2 -based

full-Heusler alloys Rh_2FeZ ($Z = \text{Ga}$ and In) [15]. Rh_2CrSb , Rh_2MnBi , Rh_2MnAl , Rh_2CrAl and Rh_2CrIn , another series of full heusler alloys, were studied by first-principles computational methods [16].

In the present work, we focused our study on the structural, electronic and magnetic properties of $\text{Rh}_2\text{CrGe}_{1-x}\text{Al}_x$ ($x = 0, 0.25, 0.50, 0.75$) compounds. The rest of the paper is arranged as follows: section 2 includes computational details and the method of calculation, section 3 is devoted to the results and discussion, and section 4 is a summary of our conclusions.

2. Computational method

We have carried out first principles calculations using the full potential linear augmented plane wave (FP-LAPW) methods [17] as implemented in the WIEN2k code [18] in the framework of the density functional theory (DFT) [19, 20] within the generalized gradient approximation (GGA-PBE) [21]. In this method, the space is divided into non-overlapping muffin-tin (MT) spheres separated by an interstitial region. In this context, the basic functions are expanded in combinations of spherical harmonic functions inside the muffin-tin spheres and Fourier series in the interstitial region. In the calculations, the Rh ($4d^8 5s^1$), Al ($3s^2 3p^1$), Cr ($3d^5 4s^1$) and Ge ($3d^1 04s^2 4p^2$) states are treated as valence electrons.

The valence wave functions inside the MT spheres are expanded in terms of spherical harmonics up to $l_{\max} = 10$. We set the parameter $RMT \cdot K_{\max} = 7$ (where RMT is the average radius of the MT spheres and K_{\max} is the largest reciprocal lattice vector used in the plane wave expansion). The magnitude of the largest vector in charge density Fourier expansion (G_{\max}) was 14 (a.u.)^{-1} . Both the plane wave cut-off and the number of k-points were varied to ensure total energy convergence. Our calculations for valence electrons were performed in a scalar-relativistic approximation, while the core electrons were treated relativistic. The self-consistent calculations were considered to converge only when the calculated total energy of the crystal converges to less than 10^{-4} Ry.

In order to simulate the $\text{Rh}_2\text{CrGe}_{1-x}\text{Al}_x$ ($x = 0.25, 0.50, 0.75$) quaternary alloy, we generate a supercell with 16 atoms. For $x = 0.25$, we substituted one atom of Ge by one atom of Al; for $x = 0.50$, we substituted two atoms of Ge by two atoms of Al; for $x = 0.75$, we substituted three atoms of Ge by three atoms of Al.

3. Results and discussion

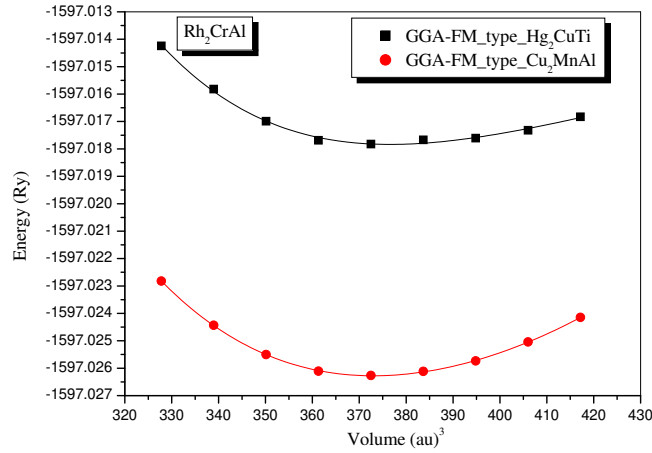
3.1. Structural properties

Heusler alloys can be classified into two main groups, namely, half-Heusler XYZ alloys and full-Heusler X_2YZ alloys. Here, X and Y denote transition metal elements, and Z is a sp -element. Full Heusler X_2YZ alloys generally have two types of structures [22, 23]. The first one is $L21$ (regular cubic phase, prototype Cu_2MnAl in which the two X atoms occupy A (0, 0, 0) and C (1/2, 1/2, 1/2) positions, and Y, Z atoms occupy B (1/4, 1/4, 1/4) and D (3/4, 3/4, 3/4) positions, respectively. The second one is XA (“inverted cubic phase”, prototype Hg_2CuTi), in which the two X atoms occupy A (0, 0, 0) and B (1/4, 1/4, 1/4) positions, and Y, Z atoms occupy C (1/2, 1/2, 1/2) and D (3/4, 3/4, 3/4) positions, respectively [23]. According to Luo *et al.* [24], the site preference of the X and Y atoms is strongly influenced by the number of their $3d$ electrons. Those elements with more $3d$ electrons prefer to occupy the A and C sites and those with fewer ones tend to occupy the B sites. As a first step, we studied the phase stability of Rh_2CrGe and Rh_2CrAl in the two types of structures and we found that Cu_2MnAl ($L21$) is more stable as shown in figure 1.

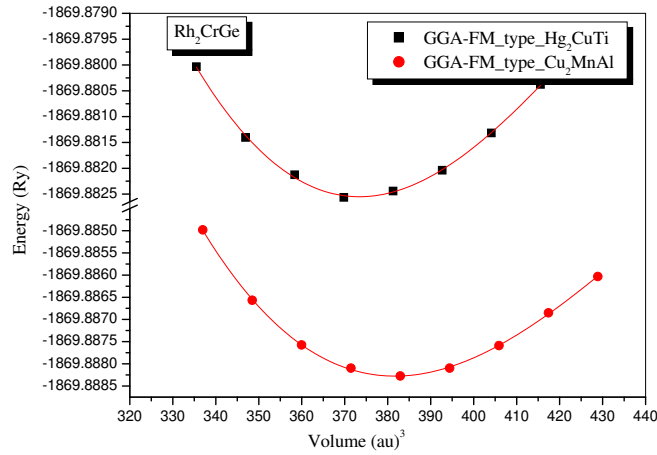
The total energy as a function of the cell volume curves was fitted to the Murnaghan equation of [25], in order to determine the ground state properties

$$E(V) = E_0(V) + \frac{BV}{B'(B' - 1)} \left[B \left(1 - \frac{V_0}{V} \right) + \left(\frac{V_0}{V} \right)^{B'} - 1 \right]. \quad (3.1)$$

Here, E_0 , V_0 , B and B' are the equilibrium energy, volume, bulk modulus and its first derivative,



(a)



(b)

Figure 1. (Colour online) Variation of the total energy as a function of the unit-cell volume of Rh_2CrGe , Rh_2CrAl for both Hg_2CuTi and Cu_2MnAl type structure.

respectively. The equilibrium structural parameters (a , B and B') of $\text{Rh}_2\text{CrGe}_{1-x}\text{Al}_x$ Heusler alloys in both Hg_2CuTi and Cu_2MnAl phases are given in table 1.

Note that for the present Heusler alloys [$\text{Rh}_2\text{CrGe}_{1-x}\text{Al}_x$ ($x = 0.25, 0.5, 0.75$)], there are no experimental or theoretical data accessible to get our calculations started. In order to obtain their approximate lattice parameters, we have applied a linear combination of the lattice constants of the $\text{Rh}_2\text{CrGe}_{1-x}\text{Al}_x$ alloys and the associated concentration x of Al incorporated atom allowing for the so-called Vegard's law [26–28].

$$\text{Rh}_2\text{CrGe}_{0.75}\text{Al}_{0.25}: a = (6.088 \times 0.75) + (6.044 \times 0.25) = 6.077 \text{ \AA},$$

$$\text{Rh}_2\text{CrGe}_{0.5}\text{Al}_{0.5}: a = (6.088 \times 0.5) + (6.044 \times 0.5) = 6.066 \text{ \AA},$$

$$\text{Rh}_2\text{CrGe}_{0.25}\text{Al}_{0.75}: a = (6.088 \times 0.25) + (6.044 \times 0.75) = 6.055 \text{ \AA}.$$

The obtained lattice parameter values for the $\text{Rh}_2\text{CrGe}_{0.75}\text{Al}_{0.25}$, $\text{Rh}_2\text{CrGe}_{0.5}\text{Al}_{0.5}$ and $\text{Rh}_2\text{CrGe}_{0.25}\text{Al}_{0.75}$ Heusler alloys are well accorded with Vegard's law values, which are higher by 0.34%, 0.32% and 0.3%, respectively.

By analyzing the present results, we can see the direct proportion between the lattice parameters

Table 1. Structural parameters (a , B and B') of Rh_2CrGe , Rh_2CrAl and $\text{Rh}_2\text{CrGe}_{1-x}\text{Al}_x$ ($x = 0.25, 0.5$ and 0.75).

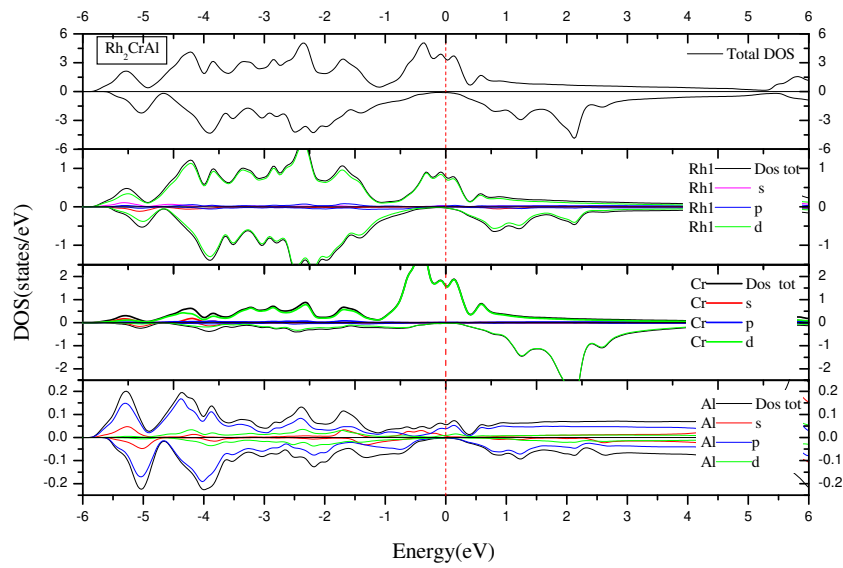
Rh_2YZ			$a(\text{\AA})$	$B(\text{GPa})$	B'
Rh_2CrGe	Cu_2MnAl Type	FM	6.936	193.715	4.95
	Hg_2CuTi Type	FM	6.046	227.177	4.155
Rh_2CrAl	Cu_2MnAl Type	FM	6.306	176.087	4.712
	Hg_2CuTi Type	FM	6.0468	200.36	4.4762
$\text{Rh}_2\text{CrGe}_{0.25}\text{Al}_{0.75}$		FM	6.0580	199.0289	4.7142
$\text{Rh}_2\text{CrGe}_{0.50}\text{Al}_{0.50}$		FM	6.0692	200.0788	4.6488
$\text{Rh}_2\text{CrGe}_{0.75}\text{Al}_{0.25}$		FM	6.0804	199.6756	4.7420

[obtained by GGA for the Cu_2MnAl ($L21$) structure and calculated by Vegard's law] of the three Heusler alloys and the concentration (x) of Al atom. This occurs owing to the Ge (125 pm) large atomic radius compared to the Al (118 pm) radius, respectively. It is clearly seen that the GGA offers greater values than the Vegard's law ones. At the same time, the corresponding bulk modulus values are 199.6756 GPa, 200.0788 GPa and 199.0289 GPa, respectively. We can conclude that $\text{Rh}_2\text{CrGe}_{0.25}\text{Al}_{0.75}$ is the most compressible full Heusler alloy.

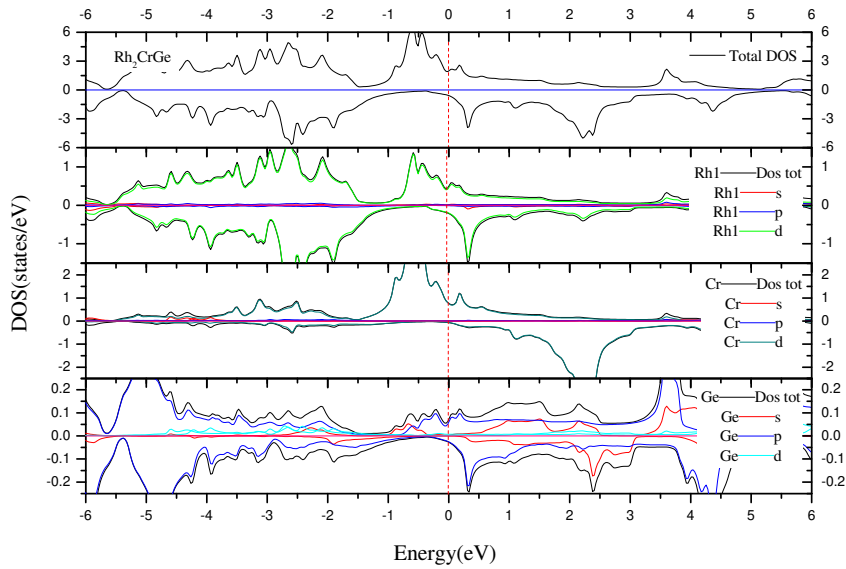
3.2. Electronic and magnetic properties

The calculated densities of states for Rh_2CrGe and Rh_2CrAl are presented in figure 2, the responsibility of transition metals $3d$ -states is very significant in the description of density of states calculations. The magnetic moments of the materials depend on the interactions of $3d$ -band structure with other states [29]. Coey *et al.* [30] have proposed a large classification scheme for half-metallic ferromagnets: A material with conducting electrons (metallic behavior) at one for the spin channels and an integer moment at $T = 0$ is a good candidate for A type-I half-metallic ferromagnet. This is the phenomenon described by de Groot *et al.* [31]. Type-IA half-metals are metallic in spin up, and semiconducting in spin down; the opposite is true for the type-IB half-metals [32]. For the Rh_2CrGe Heusler alloy, the majority-spin bands are metallic due to the overlap between the conduction and valence bands around E_F , but the minority-spin bands are nearly semiconductors because the conduction band minimum cut little the E_F at the Γ symmetry point. Thus, Rh_2CrGe is nearly half-metallic.

For Rh_2CrAl full Heusler alloys, we can see that spin up present a metallic behavior while spin down is semiconductor which indicates a half-metallic behavior. Slater and Pauling [33, 34] had exposed that for a binary magnetic alloy, when we add one valence electron in the compound, this occupies spin-down states only and the total spin magnetic moment decreases by about $1 \mu\text{B}$. For $L21$ full-Heusler, the relation between the total spin magnetic moment in the unit cell M_t and total number of valence electrons Z_t is $M_t = Z_t - 24$ [35]. The number "24" in this formula comes from the number of completely occupied minority states which consist of one s , three p and eight d states and gives total 12 states [35]. These Slater and Pauling rules join the electronic properties directly to the magnetic properties, and present a powerful tool to the study of HM Heusler compounds. The number of valence electrons Z_t for Rh_2CrAl and Rh_2CrGe is 27 [$Z_t = (9 \times 2) + 6 + 3 = 27$] and 28 [$Z_t = (9 \times 2) + 6 + 4 = 28$], respectively, their total spin magnetic moments are $3.000 \mu\text{B}$ (integer value which confirms a half-metallic behavior) and $3.97579 \mu\text{B}$ (nearly integer which confirms a nearly half-metallic behavior), respectively. The basis of the HM gap is discussed in herein below. The HM gaps frequently take place from three aspects [36]: 1) charge transfer band gap [36] which is frequently seen in CrO_2 and double perovskites [36], 2) covalent band gap which is present in the half-Heusler with $C1b$ structure, and 3) $d-d$ band gap, that is the origin



(a)

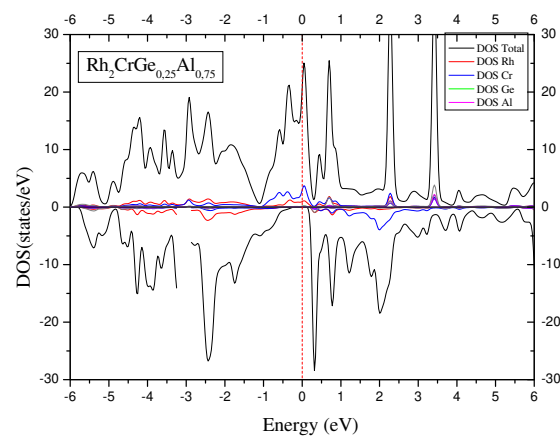


(b)

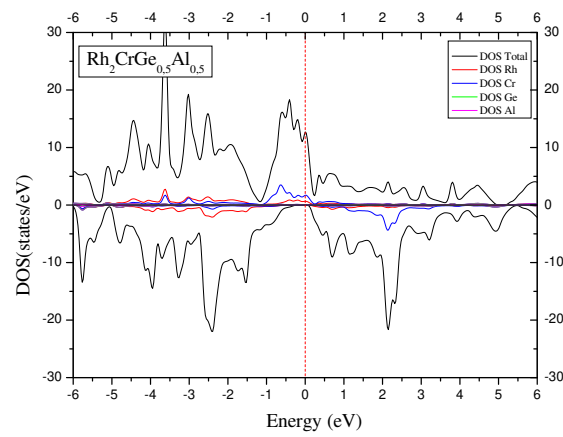
Figure 2. (Colour online) Densities of states of Rh_2CrGe and Rh_2CrAl .

of the HM band gap in the full-Heusler alloys with Cu_2MnAl structure. In the latter case, there is a quite strong hybridization between d orbitals of transition metals which makes the d -orbitals split into bonding e_g and t_{2g} orbitals below the Fermi level and anti-bonding e_g^* and t_{2g}^* orbitals above the Fermi level. This hybridization is known as $d-d$ hybridization [37].

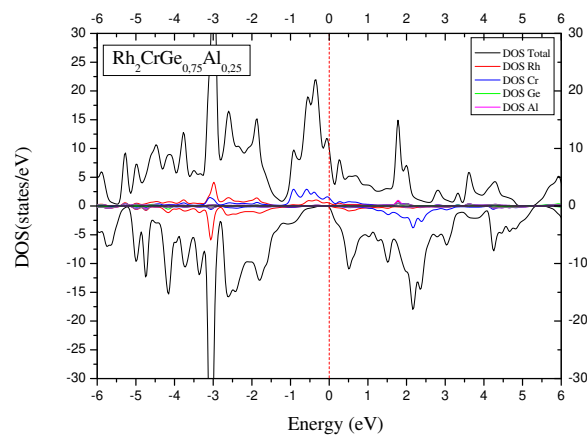
The calculated total and partial densities of state of $\text{Rh}_2\text{CrGe}_{1-x}\text{Al}_x$ ($x = 0.25, 0.5, 0.75$) compounds within the GGA approach are shown in figure 3. One can observe the absence of the gap at Fermi level in the spin (\uparrow) and its presence in spin (\downarrow), which confirms the metallic behavior for spin (\uparrow)



(a)



(b)



(c)

Figure 3. (Colour online) Total and partial densities of states of $\text{Rh}_2\text{CrGe}_{1-x}\text{Al}_x$ ($x = 0.25, 0.5$ and 0.75) compounds.

Table 2. The calculated total and partial magnetic moments (in μB) for Rh_2CrGe , Rh_2CrAl and $\text{Rh}_2\text{CrGe}_{1-x}\text{Al}_x$ ($x = 0.25, 0.5$ and 0.75) compounds.

		$M(\text{Rh}_1)$	$M(\text{Rh}_2)$	$M(\text{Cr})$	$M(\text{Ge})$	$M(\text{Al})$	M_{int}	μ Total
Rh_2CrGe	GGA-PBE	0.35055	0.35055	3.03681	-0.00748	-	0.24537	3.97579
Rh_2CrAl	GGA-PBE	0.19516	0.19516	2.57815	-0.0284	-0.06126	-	3.000
$\text{Rh}_2\text{CrGe}_{0.25}\text{Al}_{0.75}$	GGA-PBE	0.24261	0.24261	2.69551	-0.0059	-0.0256	0.34582	12.99083 (with unit cell of 16 atoms)
$\text{Rh}_2\text{CrGe}_{0.5}\text{Al}_{0.5}$	GGA-PBE	0.29814	0.29814	2.81287	-0.0041	-0.0240	0.43532	14.00174 (with unit cell of 16 atoms)
$\text{Rh}_2\text{CrGe}_{0.75}\text{Al}_{0.25}$	GGA-PBE	0.35669	0.35669	2.91783	-0.00014	-0.0237	0.51850	15.00682 (with unit cell) of 16 atoms)

and the semi-conducting behavior for spin (\downarrow). As a result, the $\text{Rh}_2\text{CrGe}_{0.25}\text{Al}_{0.75}$, $\text{Rh}_2\text{CrGe}_{0.5}\text{Al}_{0.5}$ and $\text{Rh}_2\text{CrGe}_{0.75}\text{Al}_{0.25}$ are full Heusler are half-metallic compounds. The DOS is characterized by a large domination of the Cr-3d states, which leads to the large spin moments at their sites, which are around 12.99083 μB , 14.00174 μB and 15.00682 μB for the $\text{Rh}_2\text{CrGe}_{0.25}\text{Al}_{0.75}$, $\text{Rh}_2\text{CrGe}_{0.5}\text{Al}_{0.5}$ and $\text{Rh}_2\text{CrGe}_{0.75}\text{Al}_{0.25}$ compounds, respectively as shown in table 2. It is seen that the total magnetic moment per unit cell decreases as a function of x concentration (4 μB , 15.00682 $\mu\text{B}/16$ atoms, 14.00174 $\mu\text{B}/16$ atoms, 12.990 $\mu\text{B}/16$ atoms, and 3 μB , for $x = 0, 0.25, 0.50, 0.75$, and 1, respectively), for $\text{Rh}_2\text{CrGe}_{1-x}\text{Al}_x$ ($x = 0, 0.25, 0.5, 0.75$ and 1). The calculated spin magnetic moments for the $\text{Rh}_2\text{CrGe}_{0.25}\text{Al}_{0.75}$, $\text{Rh}_2\text{CrGe}_{0.5}\text{Al}_{0.5}$ and $\text{Rh}_2\text{CrGe}_{0.75}\text{Al}_{0.25}$ alloys show that the total magnetic moment which includes the contribution from the interstitial region, comes mainly from the Cr ion with a small contribution of Rh sites. The Ge and Al atoms have a small anti-parallel spin moment to that of the Rh atom occupying the X sites in the lattice.

4. Conclusion

In this paper, we have presented theoretical results of structural, electronic and magnetic properties of $\text{Rh}_2\text{CrGe}_{1-x}\text{Al}_x$ Heusler alloys. Calculations were performed using the FP-LAPW method as implemented in WIEN2k code within GGA-PBE. The most important results are as follows:

The alloys studied are more stable in Cu_2MnAl ($L21$) structure.

The ground state properties of the materials studied are determined in the two phases.

The calculated density of state of the ferromagnetic configuration for Rh_2CrGe and Rh_2CrAl show that the first one is nearly half-metallic and the second one is half-metallic.

For $x = 0.25, 0.50$ and 0.75 , the materials have a metallic behavior for spin-up and a semi-conducting behavior for spin-down, so these materials are half-metallic compounds which are most functional in spintronic.

The magnetic moments were mostly contributed by the 3d orbital of Cr and 4d orbital of Rh ions. In the absence of experimental and theoretical works, the present results for the alloys studied provide an estimate of these materials which can be useful for further studies.

References

1. Heusler F., Starck W., Haupt E., Ber. Dtsch. Chem. Ges., 1903, **5**, 219–223.
2. Graf T., Felser C., Parkin S.S.P., Prog. Solid State Chem., 2011, **39**, 1–50, doi:10.1016/j.progsolidstchem.2011.02.001.
3. Webster P.J., Ziebeck K.R.A., In: Magnetic Alloy and Compounds of d -Elements with Main Group Elements, Wijn H.P.J. (Ed.), Landolt-Bornstein New Series Group III, **19c**, Springer, Berlin, 1988, 75.

4. Ziebeck K.R.A., Neuman K.-U., In: *Magnetic Properties of Metals*, Wijn H.P.J. (Ed.), Landolt-Bornstein New Series Group III, **32**, Springer, Berlin, 2001, 64.
5. Felser C., Fecher G.H., Balke B., *Angew. Chem. Int. Ed.*, 2007, **46**, 668, doi:10.1002/anie.200601815.
6. Shutoh N., Sakurada S., *J. Alloys Compd.*, 2005, **389**, 204, doi:10.1016/j.jallcom.2004.05.078.
7. Lue C.S., Kuo Y.-K., *Phys. Rev. B*, 2002, **66**, 085121, doi:10.1103/PhysRevB.66.085121.
8. Winterlik J., Fecher G.H., Felser C., *Solid State Commun.*, 2008, **145**, 475, doi:10.1016/j.ssc.2007.12.020.
9. Hillebrands B., Felser C., *J. Phys. D: Appl. Phys.*, 2006, **39**, 5, doi:10.1088/0022-3727/39/5/E01.
10. Yamamoto M., Marukame T., Ishikawa T., Matsuda K., Uemura T., Arita M., *J. Phys. D: Appl. Phys.*, 2006, **39**, 824, doi:10.1088/0022-3727/39/5/S08.
11. Suits J.C., *Solid State Commun.*, 1976, **18**, 423, doi:10.1016/0038-1098(76)90040-5.
12. Gupta D.C., Bhat I.H., *J. Alloys Compd.*, 2013, **575**, 292–303, doi:10.1016/j.jallcom.2013.05.185.
13. Gupta D.C., Bhat I.H., *Mater. Chem. Phys.*, 2014, **146**, 303, doi:10.1016/j.matchemphys.2014.03.027.
14. Pugaczowa-Michalska M., Jezierski A., *Physica B*, 1998, **253**, 163–167, doi:10.1016/S0921-4526(98)00364-0.
15. El Amine Monir M., Ullah H., Baltach H., Mouchaal Y., *J. Supercond. Novel Magn.*, 2018, **31**, 2233–2239, doi:10.1007/s10948-017-4499-1.
16. Gilleßen M., Dronskowski R., *J. Comput. Chem.*, 2009, **30**, 1290–1299, doi:10.1002/jcc.21152.
17. Slater J.C., *Adv. Quantum Chem.*, 1964, **1**, 5564, doi:10.1016/S0065-3276(08)60374-3.
18. Blaha P., Schwarz K., Madsen G.K.H., Kvasnicka D., Luitz J., WIEN2K, An Augmented Plane Wave Local Orbitals Program for Calculating Crystal Properties, Karlheinz Schwarz, Technische Universität, Wien, Austria, 2001.
19. Hohenberg P., Kohn W., *Phys. Rev. B*, 1964, **136**, B864, doi:10.1103/PhysRev.136.B864.
20. Kohn W., Sham L.J., *Phys. Rev. A*, 1965, **140**, A1133, doi:10.1103/PhysRev.140.A1133.
21. Perdew J., Burke K., Ernzerhof M., *Phys. Rev. Lett.*, 1996, **77**, 3865, doi:10.1103/PhysRevLett.77.3865.
22. Wang X., Cheng Z., Khenata R., Rozale H., Wang J., Wang L., Guo R., Liu G., *J. Magn. Magn. Mater.*, 2017, **423**, 285–290, doi:10.1016/j.jmmm.2016.09.043.
23. Kübler J., Fecher G.H., Felser C., *Phys. Rev. B*, 2007, **76**, 024414, doi:10.1103/PhysRevB.76.024414v.
24. Luo H.Z., Zhu Z.Y., Liu G.D., Xu S.F., Wu G.H., Liu H.Y., Qu J.P., Li Y.X., *J. Magn. Magn. Mater.*, 2008, **320**, 421, doi:10.1016/j.jmmm.2007.06.021.
25. Murnaghan F.D., *Proc. Natl. Acad. Sci. USA*, 1944, **30**, 5390.
26. Dahmane F., Khenata R., Doumi B., Bin Omran S., Kityk I.V., Sandeep C., Tadjer A., Syrotyuk S.V., Rai D.P., *J. Supercond. Novel Magn.*, 2016, **29**, 3193, doi:10.1007/s10948-016-3711-z.
27. Dahmane F., Semari F., Doumi B., Bin Omran S., Parkash D., Verma K.D., Khenata R., *Chin. J. Phys.*, 2018, **56**, 1764, doi:10.1016/j.cjph.2018.05.005.
28. Semari F., Dahmane F., Baki N., Al-Douri Y., Akbudak S., Uğur G., Uğur Ş., Bouhemadou A., Khenata R., Voon C.H., *Chin. J. Phys.*, 2018, **56**, 567–573, doi:10.1016/j.cjph.2018.01.015.
29. Rauf S., Arif S., Haneef M., Amin B., *J. Phys. Chem. Solids*, 2015, **76**, 153–169, doi:10.1016/j.jpcs.2014.07.021.
30. Coey J.M.D., Venkatesan M., Bari M.A., In: *Lecture Notes in Physics*, Vol. 595, Springer, Heidelberg, 2002, 377.
31. De Groot R.A., Mueller F.M., van Engen P.G., Buschow K.H.J., *Phys. Rev. Lett.*, 1983, **50**, 2024, doi:10.1103/PhysRevLett.50.2024.
32. Felser C., Fecher G.H., Balke B., *Angew. Chem. Int. Ed.*, 2007, **46**, 668–699, doi:10.1002/anie.200601815.
33. Slater J.C., *Phys. Rev.*, 1936, **49**, 537, doi:10.1103/PhysRev.49.537.
34. Pauling L., *Phys. Rev.*, 1938, **54**, 899, doi:10.1103/PhysRev.54.899.
35. Galanakis I., Dederichs P.H., Papanikolaou N., *Phys. Rev. B*, 2002, **66**, 174429, doi:10.1103/PhysRevB.66.174429.
36. Ahmadian F., *J. Alloys Compd.*, 2013, **576**, 279–284, doi:10.1016/j.jallcom.2013.04.159.
37. Esteki S., Ahmadian F., *J. Magn. Magn. Mater.*, 2017, **438**, 12–19, doi:10.1016/j.jmmm.2017.03.081.

Теоретичне дослідження фазової стійкості, електронних і магнітних властивостей сплавів Хеслера $Rh_2CrGe_{1-x}Al_x$ ($x = 0, 0.25, 0.50, 0.75$ і 1) методом FP-LAPW

М. Каджауд¹, М. Мохтарі^{2,3}, Л. Джоуді^{1,3}, М. Мерабе^{1,3}, С. Беналья^{1,3}, Д. Рачед¹, Р. Белачел¹, Ф. Замі⁴, Ф. Дахман³

¹ Лабораторія магнітних матеріалів, фізичний факультет, університет Сіді-Бель-Аббес, Алжир

² Університет природничих наук і технологій ім. Муххамеда Будіафа, 31000 Оран, Алжир

³ Інститут природничих наук і технологій, університетський центр м. Тіссемсілт, 38000 Тіссемсілт, Алжир

⁴ Лабораторія конденсованої речовини і сталого розвитку, фізичний факультет, університет Сіді-Бель-Аббес, Алжир

Проведено першопринципні обчислення в рамках теорії функціоналу густини з використанням методу лінеаризованих приєднаних плоских хвиль з повним потенціалом та коду WIEN2k з метою визначення структурної стійкості електронних і магнітних властивостей $Rh_2CrGe_{1-x}Al_x$ ($x = 0, 0.25, 0.50, 0.75$ і 1). Результати показали, що для Rh_2CrAl і Rh_2CrGe , структура типу Cu_2MnAl є енергетично більш стійкою, ніж структура типу Hg_2CuTi при рівноважному об'ємі. Обчислені густини станів для Rh_2CrAl і Rh_2CrGe показали, відповідно, напівметалеву та майже металеву поведінку. $Rh_2CrGe_{1-x}Al_x$ ($x = 0.25, 0.50, 0.75$) цих сплавів показали напівметалеву поведінку. Ці сполуки можна вважати хорошими кандидатами для спінтронних застосувань.

Ключові слова: сплави Хеслера, структурні властивості, електричні властивості, магнітні властивості
